

Effects of proton and metal cations on the fluorescence properties of anthracene bearing macrocyclic polyether and polyamine receptors

Yoshiko Kohno, Yasuhiro Shiraishi*, Takayuki Hirai

Research Center for Solar Energy Chemistry, and Division of Chemical Engineering, Graduate School of Engineering Science, Osaka University, Toyonaka 560-8531, Japan

Received 22 September 2007; received in revised form 15 October 2007; accepted 16 October 2007

Available online 23 October 2007

Abstract

An anthracene (AN) derivative bearing azacrown ether (1-aza-18-crown-6) and cyclen (1,4,7,10-tetraazacyclododecane) receptors (**L1**) has been synthesized. Effects of proton (H^+) and metal cations (K^+ and Zn^{2+}) on the fluorescence properties of **L1** have been studied in water and methanol. In water, H^+ addition to **L1** leads to a fluorescence intensity (I_F) increase. Potentiometrical pH titration reveals that strong I_F enhancement of **L1** requires monoprotection of both azacrown and cyclen moieties. Addition of Zn^{2+} and/or K^+ is ineffective for I_F enhancement because these cations do not coordinate with the azacrown moiety, leading to an electron transfer (ET) from the azacrown nitrogen to the photoexcited AN moiety. In methanol, the azacrown and cyclen moieties of **L1** coordinate with K^+ and Zn^{2+} , respectively. Zn^{2+} or K^+ addition to **L1** shows very small or moderate I_F enhancement because of ET from the uncoordinated azacrown or cyclen nitrogen to the excited AN. Addition of both K^+ and Zn^{2+} , however, still shows moderate I_F enhancement, although both macrocycles coordinate with the respective metal cations. *Ab initio* calculation reveals that the azacrown– K^+ coordination is weakened by an electrostatic repulsion between K^+ and Zn^{2+} within the complex. This allows ET from the azacrown nitrogen to the excited AN, resulting in an insufficient I_F enhancement.

© 2007 Elsevier B.V. All rights reserved.

Keywords: Anthracene; Azacrown ether; Cyclen; Fluorescent chemosensor

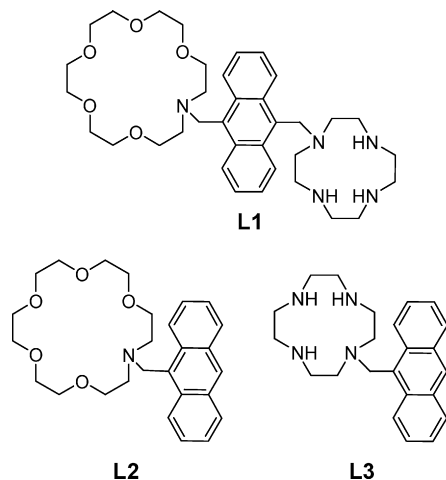
1. Introduction

There has been much interest in the development of fluorescent chemosensors because fluorometric analysis allows simple and rapid detection of chemical species in solution [1]. Considerable effort has been devoted to the development of fluorescent chemosensors for detection of pH (H^+) and metal cations [2]. The simplest sensing system for these analytes consists of a fluorophore (e.g., anthracene: AN) covalently linked to a receptor (e.g., amino group), which can bind H^+ and metal cations [2,3]. In this system, fluorescence appears when the receptor binds H^+ or metal cations. However, without H^+ and metal cations, the fluorescence is quenched by an electron transfer (ET) from the nitrogen atom of the receptor to

the photoexcited fluorophore. Among the fluorescent sensors driven by the photoinduced ET process, AN derivatives bearing an azacrown ether (1-aza-18-crown-6) receptor, **L2** [4], and bearing a cyclen (1,4,7,10-tetraazacyclododecane) receptor, **L3** [5], are known to be the fundamental and simplest sensors for detection of H^+ and metal cations. Azacrown ether behaves as a receptor for H^+ , alkali metal, alkali earth metal, and ammonium cations [6]; therefore, **L2** shows I_F enhancement upon binding these cations due to the suppression of ET from the azacrown nitrogen to the excited AN moiety [4]. In contrast, **L3** shows I_F enhancement upon binding H^+ or transition metal cations with the cyclen moiety [5,7]. So far, various fluorescent chemosensors have been synthesized based on the azacrown [8] or cyclen receptor [9]. However, a chemosensor containing both azacrown and cyclen receptors had not been proposed. In the present work, an AN-based ditopic fluorescent chemosensor (**L1**) containing both azacrown and cyclen receptors was synthesized. Effects of H^+ and metal cations (K^+ and Zn^{2+})

* Corresponding author. Tel.: +81 6 6850 6271; fax: +81 6 6850 6273.
E-mail address: shiraish@cheng.es.osaka-u.ac.jp (Y. Shiraishi).

on the fluorescence properties of **L1** were studied in water and methanol in comparison to that of the **L2** and **L3** sensors. *Ab initio* molecular orbital calculations were also performed to clarify the fluorescence property of the ditopic **L1** sensor.



2. Experimental

2.1. Synthesis

All of the reagents used were of the highest commercial quality, which were supplied from Wako and Tokyo Kasei and used without further purification. Water was purified by the Milli Q system. **L2** [4a,10] and **L3** [5a] were synthesized according to literature procedure. Synthesis route of **L1** is summarized in Scheme 1, and the detailed procedures are as follows.

2.1.1. 1-(10'-(4,7,10-tris(*tert*-Butyloxycarbonyl)-1,4,7,10-tetraazacyclododecanylmethyl)-9'-anthrylmethyl)-1-aza-4,7,10,13,16-pentaoxacyclooctadecane, **3**

L2 (0.098 g, 0.22 mmol) and paraformaldehyde (0.064 g, 0.21 mmol) were added to a mixture of acetic acid and HBr (70/30, v/v, 30 mL) and stirred at 313 K for 20 h. Water (50 mL) was added to the solution and extracted with CHCl₃ (50 mL). The resulting organic phase was dried over Na₂SO₄ and concentrated by evaporation, affording a brown viscous oil of **1** as a crude product (0.11 g) [10]. Anal. calcd. for C₂₈H₃₆NO₅Br: 546.5. MS (FAB): *m/z* 548.0 (M + H⁺). **1** (0.20 g, 0.37 mmol) and **2** [11] (0.28 g, 0.60 mmol) were refluxed with Na₂CO₃ (0.28 g, 2.6 mmol) in CHCl₃ (40 mL) for 18 h under dry N₂. The mixture was cooled to room temperature, and insoluble inorganic salt was filtered off. The resulting solution was concentrated by evaporation. *n*-Hexane and diethyl ether were added to the oily

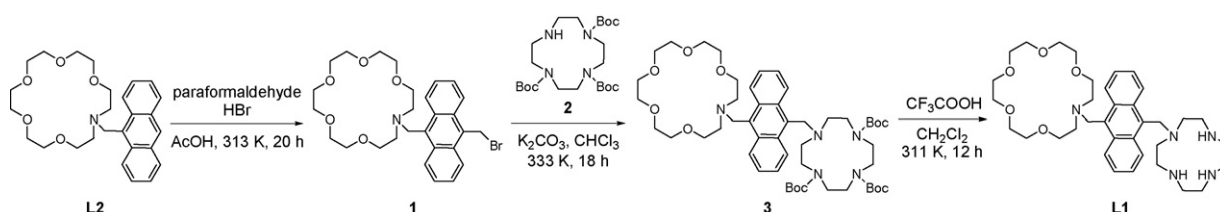
residue, and the solid formed was filtered off. The resulting solution was concentrated by evaporation, and the obtained material was purified by a silica gel column chromatography with CHCl₃ and MeOH. The later fraction was concentrated by evaporation, affording **3** as a brown solid (0.18 g, 52%). ¹H NMR (CDCl₃, 270 MHz, TMS): δ (ppm) = 1.2–1.6 (m, 27H, CH₃ of *tert*-butyloxycarbonyl), 2.4–3.8 (m, 40H, CH₂ of cyclen and crown ether), 4.6–4.8 (m, 4H, ArCH₂), 7.4 (m, 4H, ArH), 8.4–8.7 (m, 4H, ArH). ¹³C NMR (CDCl₃, 270 MHz): δ (ppm) = 28.32, 28.39, 28.46, 28.64, 49.49, 50.82, 52.01, 52.14, 53.79, 53.89, 70.05, 70.13, 70.29, 70.38, 70.47, 70.51, 70.55, 70.63, 70.72, 70.80, 79.08, 79.27, 124.08, 124.56, 124.82, 124.90, 124.99, 125.09, 125.29, 125.41, 125.68, 125.87, 127.17, 128.64, 130.99, 131.19, 155.44. Anal. calcd. for C₅₁H₇₉N₅O₁₁: 938.2. MS (FAB): *m/z* 938.7 (M⁺).

2.1.2. 1-(10'-(1,4,7,10-Tetraazacyclododecanylmethyl)-9'-anthrylmethyl)-1-aza-4,7,10,13,16-pentaoxacyclooctadecane, **L1**

A mixture of CH₂Cl₂ (10 mL) and CF₃COOH (5 mL) was added slowly to a solution of **3** (0.075 g, 8.0 μmol) dissolved in CH₂Cl₂ (10 mL) and stirred at 311 K for 12 h. The solvents were removed by evaporation. An aqueous NaOH solution (1 M, 50 mL) was added to the residue and extracted with CHCl₃ (3 × 10 mL). The combined organic phase was concentrated by evaporation. An aqueous HCl solution (0.1 M, 10 mL) was added to the residue and washed with CHCl₃. An aqueous NaOH solution (5 M, 10 mL) was then carefully added to the resulting HCl solution and extracted with CHCl₃ (3 × 10 mL). The combined organic phase was dried over Na₂SO₄ and concentrated by evaporation, affording **L1** as a brown solid (0.013 g, yield 26%): ¹H NMR (CDCl₃, 270 MHz, TMS): δ (ppm) = 2.4–3.8 (m, 40H, CH₂ of cyclen and crown ether), 4.5–4.6 (m, 4H, ArCH₂), 7.4 (m, 4H, ArH), 8.5 (m, 4H, ArH). ¹³C NMR (CDCl₃, 400 MHz): δ (ppm) = 29.67, 45.23, 45.86, 46.11, 47.08, 49.26, 53.83, 57.41, 70.19, 70.24, 70.29, 70.38, 70.51, 70.59, 70.66, 70.76, 70.87, 124.27, 125.04, 125.66, 125.92, 131.15, 133.95. Anal. calcd. for C₃₆H₅₅N₅O₅: 637.9; MS (FAB): *m/z* 638.5 (M + H⁺).

2.2. Measurements

Steady-state fluorescence spectra were measured on a Hitachi F-4500 fluorescence spectrophotometer (both excitation and emission slit widths: 2.5 nm) [12]. The measurements were carried out at 298 ± 0.1 K using a 10 mm path length quartz cell. pH of an aqueous solution was adjusted with HClO₄ and/or ben-



Scheme 1. Synthesis of **L1**.

zyltrimethylammonium hydroxide. Measurements in methanol were carried out in the presence of benzyltrimethylammonium hydroxide (10^{-3} M) as a proton scavenger [4]. KClO_4 and $\text{Zn}(\text{ClO}_4)_2$ were used as metal cations. Fluorescence quantum yields (Φ_f) were determined by comparison of the integrated corrected emission spectrum of standard quinine, which was excited at 366 nm in H_2SO_4 (0.5 M, $\Phi_f = 0.55$) [13]. Time-resolved fluorescence measurements were carried out on a PTI-3000 apparatus (Photon Technology International) using a Xe nanoflash lamp filled with N_2 as an excitation source [14] at 298 ± 0.1 K using a 10 mm path length quartz cell. Potentiometric pH titrations were carried out on a COMTITE-550 potentiometric automatic titrator (Hiranuma Co., Ltd.) with a glass electrode GE-101 [15]. Aqueous test solutions (50 mL) containing **L1** (1.5 μmol) were kept under dry N_2 in the absence or presence of metal perchlorate (1.5 μmol) with an ionic strength of $I = 0.10$ (NaClO_4). The titrations were done at 298 ± 0.1 K with an aqueous NaOH (4.65 mM) solution as a base, and at least two independent titrations were performed. Deprotonation constants and stability constants of **L1** in water were determined by means of the nonlinear least-squares program HYPERQUAD [16], where K_W ($=[\text{H}^+][\text{OH}^-]$) value used was $10^{-13.78}$ (at 298 K) [17]. Absorption spectra were recorded on an UV–vis photodiode-array spectrometer (Shimadzu; Multispec-1500) at 298 ± 0.1 K. ^1H and ^{13}C NMR spectra were obtained by a JEOL JNM-GSX270 Excalibur and JEOL JNM-AL400 using TMS as standard. The curve fitting analysis was carried out with Kaleida Graph version 3.5 (Synergy Software).

2.3. Computational details

Ab initio calculations were performed with the Gaussian 03 program package [18]. The structure optimization was carried out with the density functional theory (DFT) using the B3LYP function. The core electrons of K and Zn were replaced with the effective core potential, and their valence orbitals were described with the LANL2DZ basis set. Other atoms were calculated using the all-electron 6-31G(d) basis set. The polarized continuum model (PCM) was used for consideration of the solvent effects of methanol ($\epsilon = 32.63$). The electronically excitation energies and the oscillator strengths were calculated with the time-dependent (TD) formulation of DFT. The percentage contributions of each electronic promotion into the excited state wave function were calculated based on the largest CI coefficient expansion [19].

3. Results and discussion

3.1. pH effect in water

Effects of pH on the fluorescence properties of **L1** in water were studied in comparison to that of **L3**. Fig. 1 shows fluorescence spectra of **L1** and **L3** ($\lambda_{\text{ex}} = 366$ nm). Similar vibrational spectra were observed, where the maximum emission wavelengths were determined to be 425 (**L1**) and 417 nm (**L3**), respectively. The red-shifted fluorescence of **L1** is due to the substitution of electron-donating two methylene groups to the

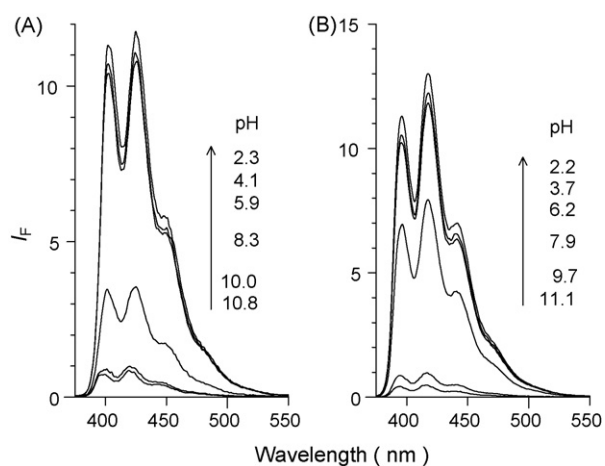


Fig. 1. pH-dependent change in fluorescence spectra ($\lambda_{\text{ex}} = 366$ nm) of (A) **L1** and (B) **L3** in aqueous solution. I_F of **L1** and **L3** obtained at pH 10 is set as 1.

AN moiety [5f]. The excitation spectra of the **L1** and **L3** fluorescence agree with the respective absorption spectra (see Supplementary material Figure S1). Fig. 2 summarizes the pH-dependent change in the fluorescence intensity (I_F) of **L1** and

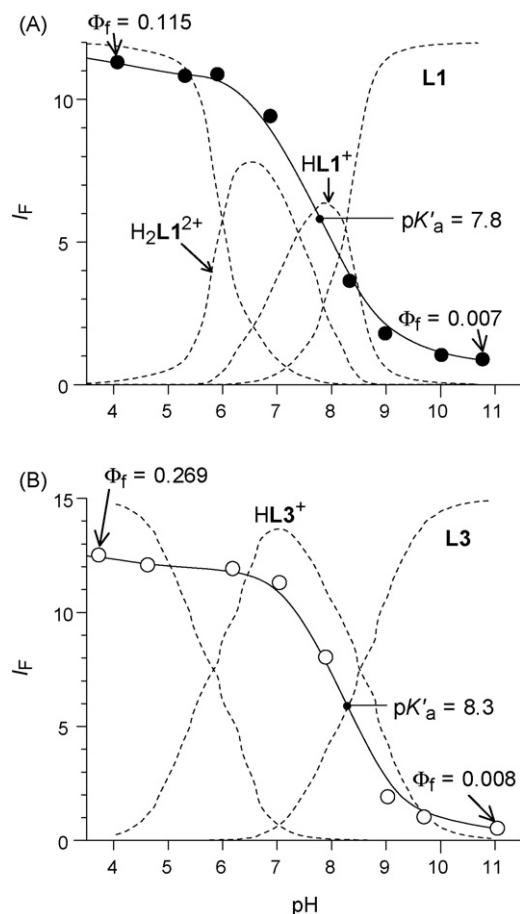


Fig. 2. pH-dependent change in I_F ($\lambda_{\text{ex}} = 366$ nm) of (A) **L1** ($\lambda_{\text{em}} = 425$ nm) and (B) **L3** ($\lambda_{\text{em}} = 417$ nm) and mole fraction distributions of their protonated states (dotted line), where tri-, tetra-, and pentaprotonated **L1** species and di-, tri-, and tetraprotonated **L3** species are shown as their total quantities. I_F of **L1** and **L3** obtained at pH 10 is set as 1.

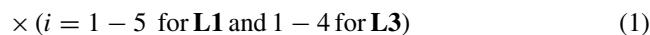
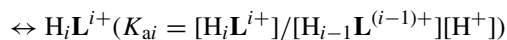
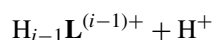
Table 1

Logarithm of the protonation constants, K_{ai} , for **L1** and **L3** determined by potentiometrical titration in water at 298 K with $I=0.10$ (NaClO₄)

	L1	L3 ^a
log K_{a1}	8.06 ± 0.28	8.41 ± 0.04
log K_{a2}	7.33 ± 0.56	5.79 ± 0.09
log K_{a3}	6.14 ± 1.08	<3
log K_{a4}	<6	<3
log K_{a5}	<6	

^a The values are from ref [5f].

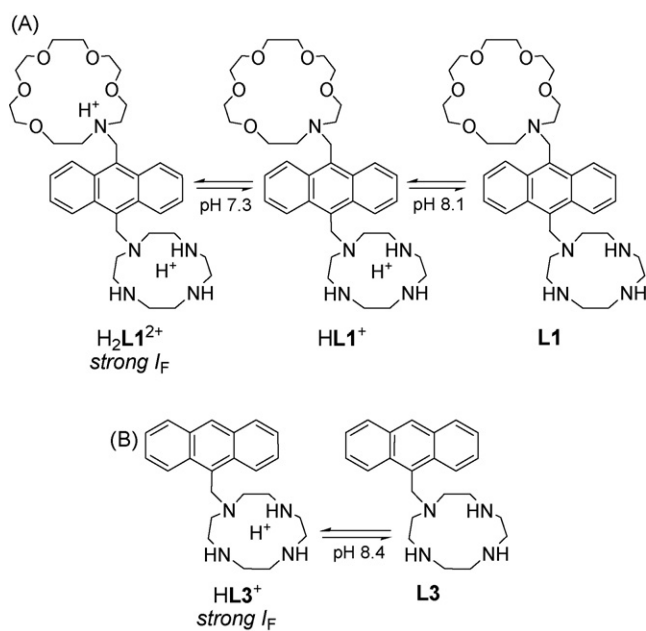
L3 (monitored at 425 nm for **L1** and 417 nm for **L3**). Both sensors demonstrate a typical sigmoidal curve. The fluorescence quenching of both sensors at basic pH (>10) is due to the ET from the unprotonated azacrown and cyclen nitrogens to the photoexcited AN moiety [4,5,20]. To clarify the relationship between I_F and the protonation states of **L1**, the potentiometric pH titration data (see Supplementary material Figure S2) were analyzed by acid–base equilibrium in Eq. (1) [17a]. The stepwise protonation constants, K_{ai} , for five nitrogens of **L1** ($i=1-5$) and four nitrogens of **L3** ($i=1-4$) were determined using the program HYPERQUAD [16].



The log K_{ai} values are summarized in Table 1, and the mole fraction distributions of the protonation states of **L1** and **L3** are shown by dotted lines in Fig. 2. Comparison of the pH– I_F profile of **L3** with the mole fraction distribution of the species (Fig. 2B) reveals that I_F increase of **L3** takes place at pH < 10, which is consistent with the formation of **HL3⁺** species. This indicates that first protonation of the cyclen nitrogen of **L3** efficiently suppresses ET to the excited AN [5f] (Scheme 2B). In contrast, as shown in Fig. 2A, **L1** shows a slight I_F increase at pH 8.5–10 (where **HL1⁺** forms mainly), while showing a drastic increase at pH < 8.5 (where **H₂L1²⁺** begins to form). As shown in Table 1, the log K_{a1} value of **L1** (8.06) is similar to that of **L3** (8.41), meaning that the first protonation of **L1** occurs on the cyclen moiety (Scheme 2A). The log K_{a2} value of **L1** (7.33) is, however, much higher than the log K_{a2} value of **L3** (5.79), but is similar to the log K_{a1} value of an AN derivative bearing two azacrown moieties (7.1) measured in a methanol/water mixture [2a]. The log K_{a2} value of **L1** is therefore assigned to the protonation of the azacrown nitrogen (Scheme 2A). These findings indicate that strong I_F enhancement of **L1** requires monoprotection of both azacrown and cyclen moieties.

3.2. Metal cation effect in water

Fig. 3 shows change in fluorescence spectra of **L1** and **L3** in aqueous solution of pH 10 with an amount of Zn²⁺ added. As shown in Fig. 3B, Zn²⁺ addition to **L3** shows I_F enhancement because Zn²⁺ coordination with the cyclen moiety suppresses ET from the cyclen nitrogen to the excited AN [5a,d]. The I_F increase



Scheme 2. Protonation sequence of (A) **L1** and (B) **L3** in water.

of **L3** becomes almost saturated upon addition of 1 equiv of Zn²⁺, indicative of 1:1 coordination of Zn²⁺ with **L3**, where the I_F enhancement is determined to be 14-fold. In contrast, as shown in Fig. 3A, **L1** shows very small I_F enhancement upon Zn²⁺ addition (1.1-fold when adding 1 equiv of Zn²⁺). Fig. 4 shows the pH– I_F profile of **L1** and **L3** measured with 1 equiv of Zn²⁺. As shown in Fig. 4B, **L3** shows I_F enhancement at pH > 8 as compared to that obtained without Zn²⁺ (bold line). However, as shown in Fig. 4A, the pH– I_F profile of **L1** is similar to that obtained without Zn²⁺ (bold line). To clarify the binding nature of Zn²⁺ with the cyclen moiety of **L1**, stability constants between the sensors and Zn²⁺, K_s , were calculated from the potentiometric pH titration data (see Supplementary material Figure S2). As summarized in Table 2, the stability constant for coordination of Zn²⁺ with the cyclen moiety of **L1** is as high as that of **L3**,

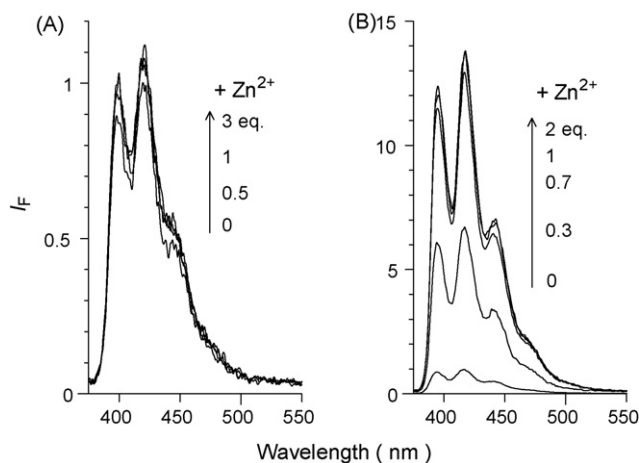


Fig. 3. Change in fluorescence spectra of (A) **L1** and (B) **L3** ($\lambda_{ex} = 366$ nm) in aqueous solution of pH 10 with the amount of Zn²⁺ added. I_F of **L1** and **L3** obtained without metal cations at pH 10 is set as 1.

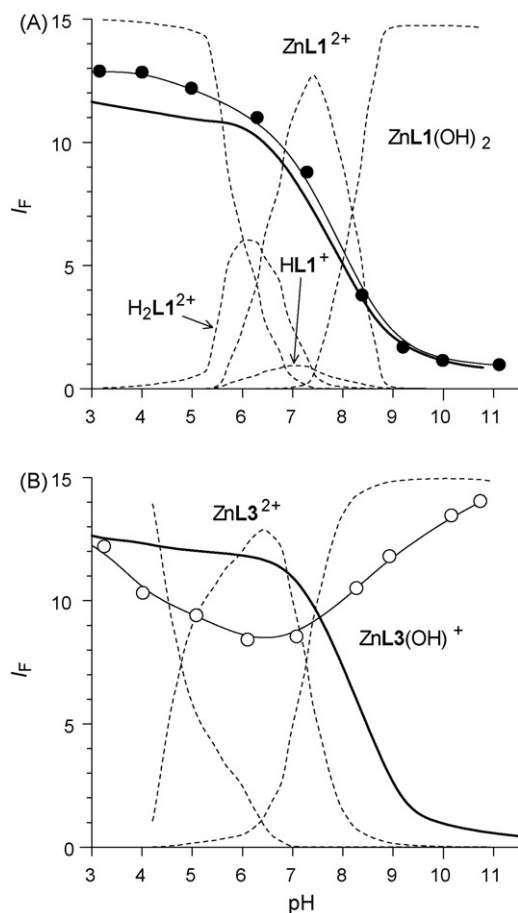


Fig. 4. pH-dependent change in I_F ($\lambda_{\text{ex}} = 366$ nm) of (A) **L1** ($\lambda_{\text{em}} = 425$ nm) and (B) **L3** [5f] ($\lambda_{\text{em}} = 417$ nm) in aqueous solution containing 1 equiv of Zn^{2+} and (dotted line) mole fraction distributions of the species, where metal-free tri-, tetra-, and pentaprotonated **L1** species and di-, tri-, and tetraprotonated **L3** species are shown as their total quantities. The bold lines in the figure denote the pH- I_F profiles for **L1** and **L3** obtained without Zn^{2+} (Fig. 2). I_F of **L1** and **L3** obtained without metal cations at pH 10 is set as 1.

indicating that the cyclen moiety of **L1** also strongly coordinates with Zn^{2+} . Fig. 4 (dotted lines) shows the mole fraction distributions of the species. As shown in Fig. 4B, at $\text{pH} > 8$, ZnL3(OH)^+ complex exists. In that, Zn^{2+} coordination with the cyclen moiety of **L3** efficiently suppresses ET from the cyclen nitrogen to the excited AN, resulting in strong I_F enhancement [5f]. In the case of **L1** (Fig. 4A), at $\text{pH} > 8$, ZnL1(OH)_2 complex exists. The very low I_F of the complex, in spite of the coordination of Zn^{2+} with the cyclen moiety, is because the ET from the uncoordinated azacrown nitrogen quenches the AN fluorescence [4]. This means that the suppression of ET from the azacrown nitrogen to

Table 2

Logarithm of the stability constants for coordination between sensors and Zn^{2+} , K_s , determined by potential titration in water at 298 K with $I = 0.10$ (NaClO_4)

Reaction	L1	L3
$\text{Zn}^{2+} + \text{L} = \text{ZnL}^{2+}$	7.34 ± 0.30	8.41 ± 0.17^a
$\text{ZnL}^{2+} + \text{OH}^- = \text{ZnL(OH)}^+$		6.62 ± 0.46
$\text{ZnL}^{2+} + 2(\text{OH}^-) = \text{ZnL(OH)}_2$	11.27 ± 0.63	

^a The value is from ref [5f].

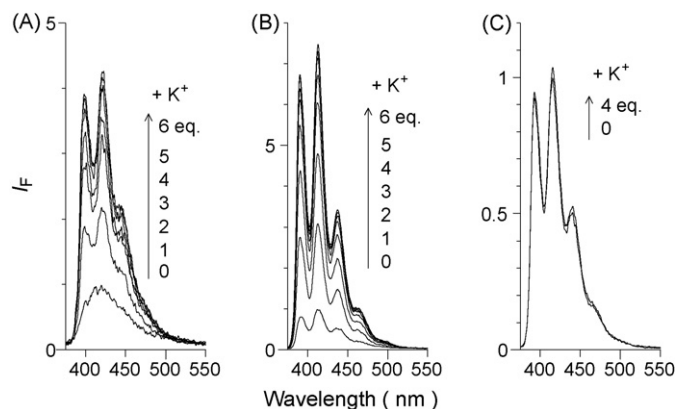


Fig. 5. Change in fluorescence spectra of (A) **L1**, (B) **L2**, and (C) **L3** ($\lambda_{\text{ex}} = 366$ nm) in methanol upon addition of K^+ . I_F of **L1**, **L2**, and **L3** obtained without metal cations is set as 1. The measurements were carried out in the presence of benzyltrimethylammonium hydroxide (10^{-3} M) as a proton scavenger.

the excited AN is the crucial factor for strong I_F enhancement of **L1**. However, crown moiety has poor binding ability to K^+ in water as well as Zn^{2+} [6a,21]. As expected, addition of K^+ or both K^+ and Zn^{2+} to an aqueous solution containing **L1** scarcely shows I_F enhancement. This suggests that the addition of these cations in water is ineffective for I_F enhancement of **L1**.

3.3. Metal cation effect in methanol

It is well-known that, in methanol, crown moiety strongly coordinates with alkali metal cations [6]. The fluorescence properties of **L1** in methanol were therefore studied. Effects of K^+ addition were studied first. As shown in Fig. 5A, addition of K^+ to a methanol solution containing **L1** shows I_F enhancement, as is also the case for **L2** (Fig. 5B) [4]. As summarized in Fig. 6A and B (black), K^+ -induced I_F enhancement of **L1** (4.2-fold when adding 6 equiv of K^+) is relatively lower than that of **L2** (7.5-fold when adding 6 equiv of K^+). To clarify the binding ability of the azacrown moiety of **L1** with K^+ , the stability constant for coordination of **L1** with K^+ , $K_s(\text{KL1}^+)$ was calculated from the fluorescence titration data with K^+ (Fig. 6, black) based on the definition in Eq. (2) [17,22].

$$\text{M}^{n+} + \text{L} \leftrightarrow \text{ML}^{n+} \quad K_s(\text{ML}^{n+}) = \frac{[\text{ML}^{n+}]}{[\text{M}^{n+}][\text{L}]} \quad (\text{M}^{-1}) \quad (2)$$

Using the total ligand concentration, $[\text{L}]_T$, the free ligand concentration, $[\text{L}]$, is expressed as Eq. (3).

$$[\text{L}] = [\text{L}]_T - [\text{ML}^{n+}] \quad (3)$$

Using the total metal cation concentration, $[\text{M}^{n+}]_T$, concentration of free metal cation, $[\text{M}^{n+}]$, is expressed as Eq. (4).

$$[\text{M}^{n+}] = [\text{M}^{n+}]_T - [\text{ML}^{n+}] \quad (4)$$

When introducing a parameter, α , defined as the ratio of $[\text{L}]$ and $[\text{L}]_T$, Eq. (2) can be expressed as Eq. (7) [22b].

$$\alpha = \frac{[\text{L}]}{[\text{L}]_T} \quad (5)$$

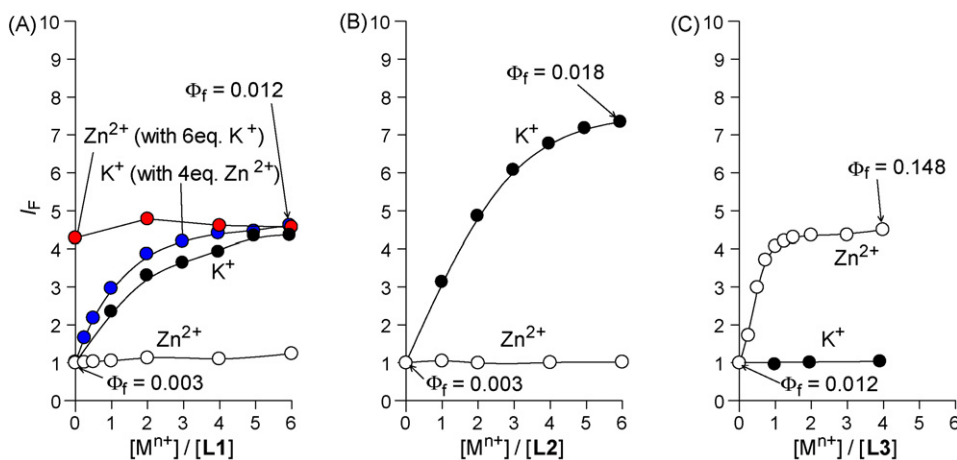


Fig. 6. Change in I_F of (A) **L1**, (B) **L2**, and (C) **L3** with the amount of Zn^{2+} and/or K^+ added [$\lambda_{em}=425$ nm (**L1**) and 417 nm (**L2** and **L3**)]. I_F of **L1**, **L2**, and **L3** obtained without metal cations is set as 1.

$$1 - \alpha = \frac{[ML^{n+}]}{[L]_T} \quad (6)$$

$$K_s[M^{n+}] = \frac{1 - \alpha}{\alpha} \quad (7)$$

When the fluorescence intensity is monitored at the same emission wavelength, α can be written as follows [22b]:

$$\alpha = \left(\frac{I_{Fmax} - I_F}{I_{Fmax} - I_{F0}} \right) \quad (8)$$

I_{F0} is the fluorescence intensity obtained without metal cations, and I_{Fmax} is the maximum fluorescence intensity where the intensity is saturated. Fig. 7A shows the plots of α versus $\log[K^+]_T$ ($\lambda_{em}=425$ nm) and the curve fitting results obtained based on Eqs. (7) and (8). As summarized in Table 3, the $\log K_s(KL1^+)$ value (5.31) is similar to that of $\log K_s(KL2^+)$ (4.91), indicating that the binding ability of the azacrown moiety of **L1** with K^+ is similar to that of **L2**. As shown in Fig. 6A and B (black), I_F enhancement of both **L1** and **L2** is almost saturated upon addition of 6 equiv of K^+ . This confirms the similar bind-

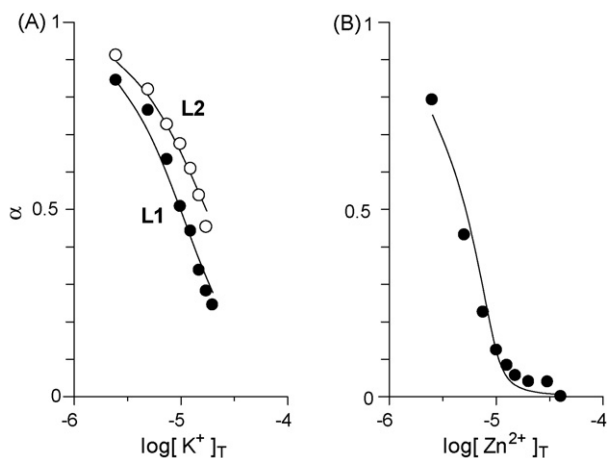


Fig. 7. Plots of the parameter, α , vs. (A) $\log[K^+]_T$ for **L1** (black) and **L2** (white) and (B) $\log[Zn^{2+}]_T$ for **L3**. The curve fitting (lines) for the experimental data (symbols) was carried out based on Eqs. (7) and (8).

Table 3

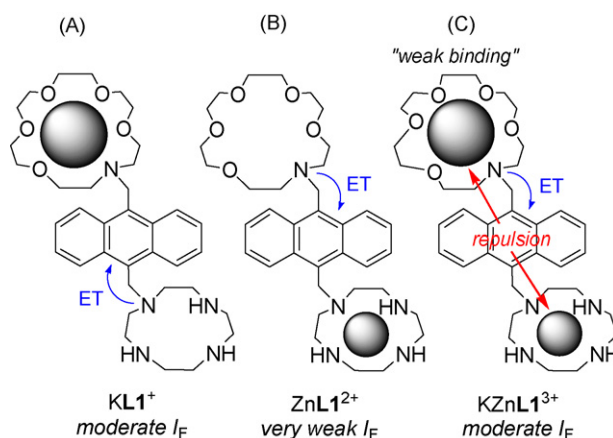
Logarithm of stability constants, K_s , for coordination between sensors and metal cations in methanol determined by the curve fitting analysis of the fluorescence titration data^a

	L1	L2	L3
$\log K_s(KL^+)$	5.31 ± 0.04	4.91 ± 0.02	
$\log K_s(ZnL^{2+})$			6.76 ± 0.28

^a The curve fitting of the fluorescence titration data were carried out based on Eqs. (7) and (8). The fitting curves are shown in Fig. 7.

ing ability of the azacrown moieties of **L1** and **L2**. The lower I_F increase of **L1** than that of **L2** upon addition of K^+ is therefore probably due to the ET from the uncoordinated cyclen nitrogen to the photoexcited AN, as summarized in Scheme 3A.

Effects of Zn^{2+} were then studied. Fig. 8 shows change in fluorescence spectra with the amount of Zn^{2+} added. As shown in Fig. 8C, Zn^{2+} addition to **L3** shows clear I_F enhancement, indicating that the cyclen– Zn^{2+} coordination suppresses the ET from the cyclen nitrogen, as is also the case in water (Fig. 3B). As summarized in Fig. 6C (white), I_F enhancement of **L3** becomes almost saturated upon addition of 1 equiv of Zn^{2+} , implying that the cyclen– Zn^{2+} binding in methanol takes place quantita-



Scheme 3. Schematic representation of fluorescence properties of **L1** complexes.

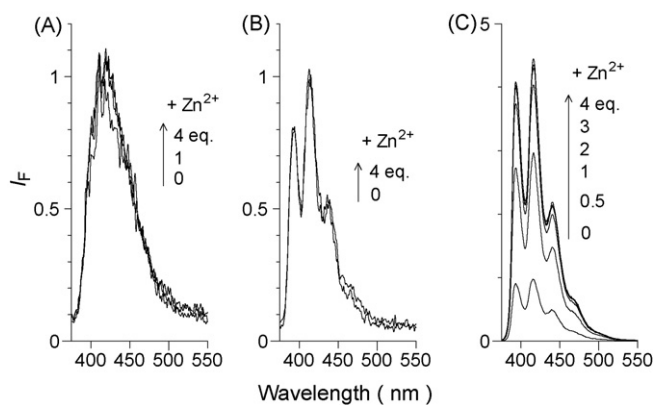


Fig. 8. Change in fluorescence spectra of (A) **L1**, (B) **L2**, and (C) **L3** ($\lambda_{ex} = 366$ nm) in methanol upon addition of Zn^{2+} . I_F of **L1**, **L2**, and **L3** obtained without metal cations is set as 1.

tively, as is also the case in water. As summarized in Table 3, the $\log K_s(ZnL3^{2+})$ value is determined by the curve fitting analysis to be 6.76, indicating that the cyclen moiety of **L3** strongly coordinates with Zn^{2+} in methanol. In contrast, as shown in Fig. 8A, addition of Zn^{2+} to **L1** shows very small I_F enhancement (1.1-fold when adding 1 equiv of Zn^{2+}). ESI mass analysis [23] of a methanol solution containing **L1** and 1 equiv of $ZnCl_2$ (see Supporting Information Figure S3) shows a strong peak at m/z 739.3, assigned to $[ZnL1 + Cl]^+$ ion, indicating that the cyclen moiety of **L1** coordinates with Zn^{2+} . As shown in Fig. 8B, addition of Zn^{2+} to **L2** does not show any fluorescence response. This suggests that the very low I_F enhancement of **L1** even upon coordination with Zn^{2+} (Fig. 8A) is due to the ET from the uncoordinated azacrown nitrogen to the excited AN (Scheme 3B), as is also the case in water.

Effects of addition of both K^+ and Zn^{2+} were then studied. Fig. 9A shows change in fluorescence spectra obtained upon addition of K^+ to a solution containing **L1** and 4 equiv of Zn^{2+} . As summarized in Fig. 6A (blue), I_F increase is larger than that obtained without Zn^{2+} (black), but the increase becomes smaller

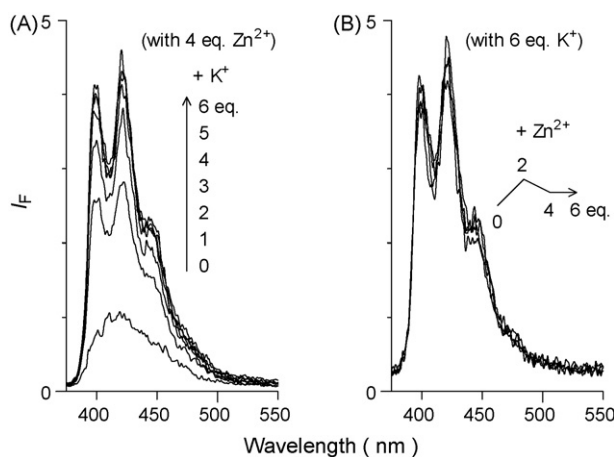


Fig. 9. Change in fluorescence spectra of **L1** ($\lambda_{ex} = 366$ nm) obtained (A) upon addition of K^+ to a methanol solution containing **L1** and 4 equiv of Zn^{2+} and (B) upon addition of Zn^{2+} to a methanol solution containing **L1** and 6 equiv of K^+ . I_F of **L1** obtained without metal cations is set as 1.

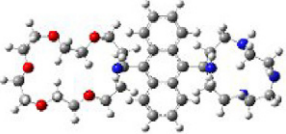
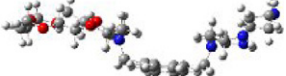

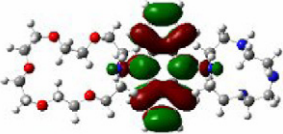

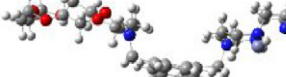
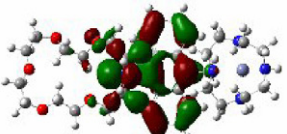

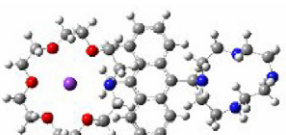
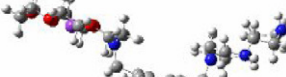
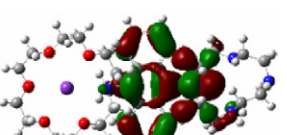
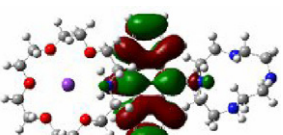
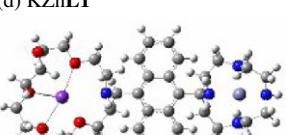
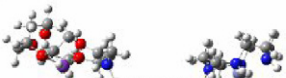
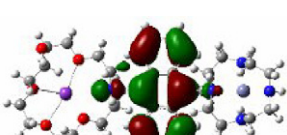
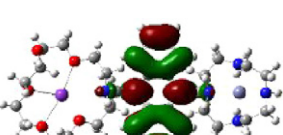
with increasing the K^+ amount; I_F obtained with 6 equiv of K^+ (blue) is similar to that obtained without Zn^{2+} (black). Fig. 9B shows change in fluorescence spectra upon addition of Zn^{2+} to a solution containing **L1** and 6 equiv of K^+ . As shown in Fig. 6A (red), Zn^{2+} addition scarcely affects I_F . In both cases containing K^+ and Zn^{2+} together (Fig. 6A, blue and red), the azacrown and cyclen moieties of **L1** probably coordinate with the respective K^+ and Zn^{2+} cations ($KZnL1^{3+}$ complex formation), which might lead to the suppression of ET from both azacrown and cyclen nitrogens. However, in both cases with 6 equiv of K^+ and 4 equiv of Zn^{2+} (Fig. 6A, blue and red), I_F is similar to that obtained only with 6 equiv of K^+ (black). Time-resolved fluorescence measurements reveal that the **L1** solution containing 6 equiv of K^+ ($KL1^+$ complex) shows a fluorescence with 1.5 ns lifetime, while the solution containing 6 equiv of K^+ and 4 equiv of Zn^{2+} together ($KZnL1^{3+}$ complex) shows a fluorescence with 2.4 ns lifetime, indicating that the respective emissions originate from the different species. This finding suggests that the $KZnL1^{3+}$ complex actually forms in solution, although the complex shows I_F similar to that of the $KL1^+$ complex.

3.4. Computational analysis of fluorescence behavior

To clarify the reason for very weak I_F of the $KZnL1^{3+}$ complex, *ab initio* calculations were performed with the Gaussian 03 program (see 2.3 Computational details) [18]. The geometry optimization was performed using the DFT theory with the B3LYP/LANL2DZ/6-31G(d) basis. The excitation energies and the oscillator strengths of the compounds were calculated with the TD-DFT theory. The optimized geometry and the interfacial plots of HOMO and LUMO orbitals of the free **L1** and its complexes are shown in Table 4, where the electronic transition properties of these compounds are summarized in Table S1 (see Supplementary material). The first electronic transition of the free **L1** and the complexes ($ZnL1^{2+}$, $KL1^+$, and $KZnL1^{3+}$) corresponds to a HOMO-LUMO transition, as is also the case for the free **L2** and **L3** and their complexes (see Supplementary material Tables S3 and S5). As shown in Table 4a, the electron density of LUMO orbital of the free **L1** is located on the AN moiety, showing a π^* electronic character. In contrast, HOMO orbital of the free **L1** has lone pair electrons on the azacrown and the benzylic cyclen nitrogens together with π -electron on the AN moiety. The appearance of the lone pair electrons [24] clearly indicates that, without metal cations, the ET from the azacrown and the benzylic cyclen nitrogens to the excited AN actually suppresses the **L1** fluorescence.

Upon coordination of Zn^{2+} with **L1** ($ZnL1^{2+}$ complex), as shown in Table 4b, the lone pair electron density on the benzylic cyclen nitrogen of the HOMO orbital is drastically reduced. In the case of **L3** (see Supplementary material Table S4), similar decrease in the lone pair electron density on the benzylic cyclen nitrogen is observed upon Zn^{2+} coordination. This indicates that the Zn^{2+} coordination with the cyclen moiety of **L1** actually suppresses the ET from the cyclen nitrogen to the AN moiety. However, as shown in Table 4b, uncoordinated azacrown nitrogen of the $ZnL1^{2+}$ complex still has a lone pair electron on the

Table 4
Geometry optimized structures and HOMO and LUMO orbitals of **L1** and its complexes determined by *ab initio* calculation^a

Geometry optimized structure		HOMO	LUMO
Top view	Side view		
(a) L1			
			
(b) ZnL1²⁺			
			
(c) KL1⁺			
			
(d) KZnL1³⁺			
			

^a Green and deep red parts on HOMO and LUMO orbitals refer to the different phases of the molecular wave functions, where the isovalue is 0.02 a.u. [18b].

HOMO orbital. This allows the ET from the azacrown nitrogen to the AN moiety, thus resulting in emission quenching (Fig. 6A, white; Scheme 3B). Upon coordination of K⁺ with **L1** (**KL1⁺** complex), as shown in Table 4c, the electron density on the azacrown nitrogen of the HOMO orbital decreases, as is also the case for **L2** (see Supplementary material Table S2). However, the uncoordinated cyclen nitrogen still has a lone pair electron on the HOMO orbital (Table 4c). This allows the ET from the cyclen nitrogen within the **KL1⁺** complex (Scheme 3A), resulting in lower I_F enhancement than the **KL2⁺** complex (Fig. 6A and B, black).

In contrast, upon addition of both Zn²⁺ and K⁺ to **L1** (**KZnL1³⁺** complex), as shown in Table 4d, electron density on the HOMO orbital is located on the azacrown nitrogen, while the electron on the cyclen nitrogen almost disappears. This means that, within the **KZnL1³⁺** complex, ET occurs from the azacrown nitrogen to the excited AN, although the azacrown moiety coordinates with K⁺. The appearance of the lone pair electron on the azacrown nitrogen of the **KZnL1³⁺** complex is explained by the weak coordination of K⁺ with the azacrown moiety due to the adjacent cyclen–Zn²⁺ complex. As shown in Table 4d (side view), the azacrown–K⁺ moiety of the **KZnL1³⁺** complex is significantly distorted as compared to that of the free **L1** and the **ZnL1²⁺** and **KL1⁺** complexes. Neither free **L2**

nor **KL2⁺** complex shows such distortion (see Supplementary material Tables S2 and S4), meaning that the distortion of the azacrown–K⁺ moiety of the **KZnL1³⁺** complex is triggered by the presence of the adjacent cyclen–Zn²⁺ moiety. This is probably due to the electrostatic charge-charge repulsion occurring between the Zn²⁺ and K⁺ cations within the complex [25]. As shown in Table 3, the stability constant for cyclen–Zn²⁺ coordination of **L3** is larger than that for azacrown–K⁺ coordination of **L1**, indicating that the cyclen–Zn²⁺ complex within **KZnL1³⁺** is more stable. As a result of this, K⁺ is forced to stay away from Zn²⁺, and hence, leads to the distortion of the azacrown moiety. The distance between K⁺ and the azacrown nitrogen within the **KZnL1³⁺** complex is determined to be 3.16 Å, which is longer than that within the **KL1⁺** complex (3.10 Å), confirming the weak binding of K⁺ and azacrown moiety within **KZnL1³⁺** [9f]. Consequently, lone pair electron is located on the azacrown nitrogen of the HOMO orbital (Table 4d), leading to ET from the azacrown nitrogen to the excited AN moiety (Scheme 3C). These are the reason for low I_F of the **KZnL1³⁺** complex (Fig. 6A, blue and red). The obtained findings demonstrate that, for the design of the ditopic fluorescent chemosensor containing both azacrown and cyclen receptors, location of these receptors and their distance are the important factors for strong fluorescence enhancement.

4. Conclusion

An anthracene (AN) derivative bearing azacrown and cyclen receptors (**L1**) has been synthesized. Effects of H^+ and metal cations (K^+ and Zn^{2+}) on the fluorescence properties of **L1** were studied in water and methanol, with the following results:

- (1) In water, fluorescence intensity (I_F) of **L1** increases with a pH decrease. Strong I_F enhancement of **L1** takes place upon monoprotation of both azacrown and cyclen moieties of **L1**, leading to suppression of electron transfer (ET) to the photoexcited AN moiety. Addition of K^+ and/or Zn^{2+} , however, scarcely leads to I_F enhancement. This is because neither K^+ nor Zn^{2+} coordinates with the azacrown moiety, thus allowing ET from the uncoordinated azacrown nitrogen to the excited AN moiety.
- (2) In methanol, the azacrown and cyclen receptors of **L1** coordinate with K^+ and Zn^{2+} , respectively. Addition of Zn^{2+} or K^+ to **L1** leads to very small or moderate I_F enhancement because of ET from the uncoordinated azacrown or cyclen nitrogen to the excited AN, indicating that the suppression of ET from the both nitrogens is important for strong I_F enhancement. Addition of both K^+ and Zn^{2+} is, however, ineffective. This is because the electrostatic repulsion between K^+ and Zn^{2+} weakens the azacrown- K^+ binding, thus allowing ET from the azacrown nitrogen to the excited AN.

Acknowledgments

We are grateful for financial support from the Grant-in-Aids for Scientific Research (No. 19760536) from the Ministry of Education, Culture, Sports, Science and Technology, Japan (MEXT). Y.K. acknowledges The Global COE (Center of Excellence) Program “Global Education and Research Center for Bio-Environmental Chemistry” of Osaka University.

Appendix A. Supplementary data

Supplementary data associated with this article can be found, in the online version, at doi:10.1016/j.jphotochem.2007.10.013.

References

- [1] A.W. Czarnik, *Fluorescent Chemosensors for Ion and Molecule Recognition*, American Chemical Society, Washington DC, 1993.
- [2] (a) R.A. Bissell, E. Calle, A.P. de Silva, S.A. de Silva, H.Q.N. Gunaratne, J.-L. Habib-Jiwan, S.L.A. Peiris, R.A.D.D. Rupasinghe, T.K.S.D. Samarasinghe, K.R.A.S. Sandanayake, J.-P. Soumillion, *J. Chem. Soc., Perkin Trans. 2* (1992) 1559–1564; (b) L. Fabbrizzi, A. Poggi, *Chem. Soc. Rev.* (1995) 197–202; (c) A.W. Czarnik, *Acc. Chem. Res.* 27 (1994) 302–308; (d) A.P. de Silva, H.Q.N. Gunaratne, T. Gunnlaugsson, A.J.M. Huxley, C.P. McCoy, J.T. Rademacher, T.E. Rice, *Chem. Rev.* 97 (1997) 1515–1566; (e) L. Fabbrizzi, M. Licchelli, L. Parodi, A. Poggi, A. Taglietti, *J. Fluoresc.* 8 (1998) 263–271; (f) B. Valeur, I. Leray, *Coord. Chem. Rev.* 205 (2000) 3–40; (g) A.P. de Silva, D.B. Fox, A.J.M. Huxley, T.S. Moody, *Coord. Chem. Rev.* 205 (2000) 41–57.
- [3] (a) A.P. de Silva, R.A.D.D. Rupasinghe, *J. Chem. Soc., Chem. Commun.* (1985) 1669–1670; (b) S.A. de Silva, A. Zavaleta, D.E. Baron, O. Allam, E.V. Isidor, N. Kashimura, J.M. Percarpio, *Tetrahedron Lett.* 38 (1997) 2237–2240; (c) M.A. Bernardo, F. Pina, B. Escuder, E. García-España, M.L. Godino-Salido, J. Latorre, S.V. Luis, J.A. Ramírez, C. Soriano, *J. Chem. Soc., Dalton Trans.* (1999) 915–921; (d) G. Greiner, I. Maier, *J. Chem. Soc., Perkin Trans. 2* (2002) 1005–1011.
- [4] (a) A.P. de Silva, S.A. de Siva, *J. Chem. Soc., Chem. Commun.* (1986) 1709–1710; (b) J.S. Benco, H.A. Nienaber, K. Dennen, W.G. McGimpsey, *J. Photochem. Photobiol. A: Chem.* 152 (2002) 33–40.
- [5] (a) E.U. Akkaya, M.E. Huston, A.W. Czarnik, *J. Am. Chem. Soc.* 112 (1990) 3590–3593; (b) M.E. Huston, C. Engleman, A.W. Czarnik, *J. Am. Chem. Soc.* 112 (1990) 7054–7056; (c) S. Charles, F. Dubois, S. Yunus, E.V. Donckt, *J. Fluoresc.* 10 (2000) 99–105; (d) S. Aoki, S. Kaido, H. Fujioka, E. Kimura, *Inorg. Chem.* 42 (2003) 1023–1030; (e) Y. Shiraishi, Y. Kohno, T. Hirai, *Ind. Eng. Chem. Res.* 44 (2005) 847–851; (f) Y. Shiraishi, Y. Kohno, T. Hirai, *J. Phys. Chem. B* 109 (2005) 19139–19147.
- [6] (a) H.K. Frensdorff, *J. Am. Chem. Soc.* 93 (1971) 600–606; (b) D.M. Dishong, G.W. Gokel, *J. Org. Chem.* 47 (1982) 147–148; (c) J.-M. Lehn, *Angew. Chem., Int. Ed. Engl.* 27 (1988) 89–112; (d) G.W. Gokel, *Crown Ethers and Cryptands*, The Royal Society Chemistry, London, England, 1991; (e) E.C. Constable, *Coordination Chemistry of Macrocyclic Compounds*, Oxford University Press, Oxford, 1999; (f) G.W. Gokel, W.M. Leevy, M.E. Weber, *Chem. Rev.* 104 (2004) 2723–2750.
- [7] (a) M. Kodama, E. Kimura, *J. Chem. Soc., Chem. Commun.* (1975) 326–327; (b) M. Kodama, E. Kimura, *J. Chem. Soc., Dalton Trans.* (1977) 2269–2276.
- [8] (a) K. Kubo, T. Sakurai, *Chem. Lett.* (1996) 959–960; (b) J.H.R. Tucker, H. Bouas-Laurent, P. Marsau, S.W. Riley, J.-P. Desvergne, *Chem. Commun.* (1997) 1165–1166; (c) J. Hua, Y.-G. Wang, *Chem. Lett.* 34 (2005) 98–99; (d) M. Baruah, W. Qin, R.A.L. Vallée, D. Beljonne, T. Rohand, W. Dehaen, N. Boens, *Org. Lett.* 7 (2005) 4377–4380.
- [9] (a) T. Hirano, K. Kikuchi, Y. Urano, T. Higuchi, T. Nagano, *Angew. Chem., Int. Ed.* 39 (2000) 1052–1054; (b) S. Mizukami, T. Nagano, Y. Urano, A. Odani, K. Kikuchi, *J. Am. Chem. Soc.* 124 (2002) 3920–3925; (c) S.C. Burdette, S.J. Lippard, *Inorg. Chem.* 41 (2002) 6816–6823; (d) S. Aoki, D. Kagata, M. Shiro, K. Takeda, E. Kimura, *J. Am. Chem. Soc.* 126 (2004) 13377–13390; (e) N.C. Lim, J.V. Schuster, M.C. Porto, M.A. Tanudra, L. Yao, H.C. Freake, C. Brückner, *Inorg. Chem.* 44 (2005) 2018–2030; (f) N.B. Sankaran, P.K. Mandal, B. Bhattacharya, A. Samanta, *J. Mater. Chem.* 15 (2005) 2854–2859; (g) R. Bozio, E. Cecchetto, G. Fabbrini, C. Ferrante, M. Maggini, E. Menna, D. Pedron, R. Riccò, R. Signorini, M. Zerbetto, *J. Phys. Chem. A* 110 (2006) 6459–6464.
- [10] B. Bag, P.K. Bharadwaj, *Chem. Commun.* (2005) 513–515.
- [11] E. Kimura, S. Aoki, T. Koike, M. Shiro, *J. Am. Chem. Soc.* 119 (1997) 3068–3076.
- [12] (a) X. Zhang, Y. Shiraishi, T. Hirai, *Tetrahedron Lett.* 48 (2007) 5455–5459; (b) Y. Shiraishi, H. Maehara, K. Ishizumi, T. Hirai, *Org. Lett.* 9 (2007) 3125–3128.
- [13] (a) W.H. Melhuish, *J. Phys. Chem.* 65 (1961) 229–235; (b) A.T.R. Williams, S.A. Winfield, *Analyst* 108 (1983) 1067–1071; (c) Y. Shiraishi, H. Koizumi, T.J. Hirai, *Phys. Chem. B* 109 (2005) 8580–8586;

- (d) H. Koizumi, Y. Shiraishi, S. Tojo, M. Fujitsuka, T. Majima, T. Hirai, J. Am. Chem. Soc. 128 (2006) 8751–8753;
- (e) H. Koizumi, Y. Kimata, Y. Shiraishi, T. Hirai, Chem. Commun. (2007) 1846–1848.
- [14] (a) Y. Shiraishi, K. Ishizumi, G. Nishimura, T. Hirai, J. Phys. Chem. B 111 (2007) 8812–8822;
- (b) Y. Shiraishi, Y. Tokitoh, G. Nishimura, T. Hirai, J. Phys. Chem. B 111 (2007) 5090–5100.
- [15] (a) G. Nishimura, K. Ishizumi, Y. Shiraishi, T. Hirai, J. Phys. Chem. B 110 (2006) 21596–21602;
- (b) Y. Shiraishi, Y. Tokitoh, T. Hirai, Chem. Commun. (2005) 5316–5318.
- [16] P. Gans, A. Sabatini, A. Vacca, Talanta 43 (1996) 1739–1753.
- [17] (a) A.E. Martell, R.J. Motekaitis, Determination and Use of Stability Constants, second ed., VCH, New York, 1992;
- (b) C.F. Baes Jr., R.E. Mesmer, The Hydrolysis of Cations, John Wiley & Sons, New York, 1976.
- [18] (a) M.J. Frisch, G.W. Trucks, H.B. Schlegel, G.E. Scuseria, M.A. Robb, J.R. Cheeseman, J.A. Montgomery Jr., T. Vreven, K.N. Kudin, J.C. Burant, J.M. Millam, S.S. Iyengar, J. Tomasi, V. Barone, B. Mennucci, M. Cossi, G. Scalmani, N. Rega, G.A. Petersson, H. Nakatsuji, M. Hada, M. Ehara, K. Toyota, R. Fukuda, J. Hasegawa, M. Ishida, T. Nakajima, Y. Honda, O. Kitao, H. Nakai, M. Klene, X. Li, J.E. Knox, H.P. Hratchian, J.B. Cross, V. Bakken, C. Adamo, J. Jaramillo, R. Gomperts, R.E. Stratmann, O. Yazyev, A.J. Austin, R. Cammi, C. Pomelli, J.W. Ochterski, P.Y. Ayala, K. Morokuma, G.A. Voth, P. Salvador, J.J. Dannenberg, V.G. Zakrzewski, S. Dapprich, A.D. Daniels, M.C. Strain, O. Farkas, D.K. Malick, A.D. Rabuck, K. Raghavachari, J.B. Foresman, J.V. Ortiz, Q. Cui, A.G. Baboul, S. Clifford, J. Cioslowski, B.B. Stefanov, G. Liu, A. Liashenko, P. Piskorz, I. Komaromi, R.L. Martin, D.J. Fox, T. Keith, M.A. Al-Laham, C.Y. Peng, A. Nanayakkara, M. Challacombe, P.M.W. Gill, B. Johnson, W. Chen, M.W. Wong, C. Gonzalez, J.A. Pople, Gaussian 03. Revision B. 05, Gaussian, Inc., Wallingford, CT, 2004;
- (b) I.I. Dennington, T. Keith, J. Millam, K. Eppinnett, W.L. Hovell, R. Gilliland, GaussView. Version 3.09, Semichem, Inc., Shawnee Mission, KS, 2003.
- [19] J. Karpiuk, Y.N. Svartsov, J. Nowacki, Phys. Chem. Chem. Phys. 7 (2005) 4070–4081.
- [20] (a) Y. Shiraishi, Y. Tokitoh, G. Nishimura, T. Hirai, Org. Lett. 7 (2005) 2611–2614;
- (b) G. Nishimura, Y. Shiraishi, T. Hirai, Chem. Commun. (2005) 5313–5315.
- [21] (a) P. Kele, J. Orbulescu, T.L. Calhoun, R.E. Gawley, R.M. Leblanc, Tetrahedron Lett. 43 (2002) 4413–4416;
- (b) R.E. Gawley, S. Pinet, C.M. Cardona, P.K. Datta, T. Ren, W.C. Guida, J. Nydick, R.M. Leblanc, J. Am. Chem. Soc. 124 (2002) 13448–13453.
- [22] (a) S. Fery-Forgues, M.-T. Le Bris, J.-P. Guetté, B. Valeur, J. Phys. Chem. 92 (1988) 6233–6237;
- (b) R.H. Yang, K.A. Li, K.M. Wang, F.L. Zhao, N. Li, F. Liu, Anal. Chem. 75 (2003) 612–621;
- (c) N. Shao, Y. Zhang, S.M. Cheung, R.H. Yang, W.H. Chan, T. Mo, K.A. Li, F. Liu, Anal. Chem. 77 (2005) 7294–7303.
- [23] (a) R. Colton, S. Mitchell, J.C. Traeger, Inorg. Chim. Acta 231 (1995) 87–93;
- (b) J.Y. Kwon, Y.J. Jang, Y.J. Lee, K.M. Kim, M.S. Seo, W. Nam, J. Yoon, J. Am. Chem. Soc. 127 (2005) 10107–10111.
- [24] H. Salman, S. Tal, Y. Chuvilov, O. Solovey, Y. Abraham, M. Kapon, K. Suwinska, Y. Eichen, Inorg. Chem. 45 (2006) 5315–5320.
- [25] J.-E. Jee, M.C. Chang, C.-H. Kwak, Inorg. Chem. Commun. 7 (2004) 614–617.